

**DESIGN OF OPTIMISED PLATE VELOCITY CONTROLLER
OF A LABORATORY SCALE ROT USING AN EHAS**

*Thesis submitted in partial fulfilment of
The requirements for the degree of*
Master of Mechanical Engineering

By

SOHAG SUTAR

Examination Roll No.: M4MEC19006

Registration No.: 119983 of 2012 - 2013

Under the guidance of

Prof. Dipankar Sanyal

&

Dr. Pranibesh Mandal

**DEPARTMENT OF MECHANICAL ENGINEERING
FACULTY OF ENGINEERING & TECHNOLOGY
JADAVPUR UNIVERSITY
KOLKATA – 700032**

2019

FACULTY OF ENGINEERING AND TECHNOLOGY
DEPARTMENT OF MECHANICAL ENGINEERING
JADAVPUR UNIVERSITY
KOLKATA

DECLARATION OF ORIGINALITY AND COMPLIANCE OF
ACADEMIC ETHICS

I hereby declare that this thesis contains literature survey and original research work, by the undersigned candidate, as part of my **Master of Mechanical Engineering** course during academic session 2017-2019.

All information in this document have been obtained and presented in accordance with academic rules and ethical conduct.

I also declare that, as required by these rules and conduct, I have fully cited and referenced all material and results that are not original to this work.

Name: SOHAG SUTAR

Examination Roll No.: M4MEC19006

Thesis Title: Design of optimised plate velocity controller of a laboratory scale ROT using an EHAS

**FACULTY OF ENGINEERING AND TECHNOLOGY
DEPARTMENT OF MECHANICAL ENGINEERING
JADAVPUR UNIVERSITY
KOLKATA**

CERTIFICATE OF APPROVAL

The foregoing thesis entitled “DESIGN OF OPTIMISED PLATE VELOCITY CONTROLLER OF A LABORATORY SCALE ROT USING AN EHAS” is hereby approved as credible study of Fluid Mechanics and Hydraulics Engineering and presented in a manner satisfactory to warrant its acceptance as a pre-requisite to the degree for which it has been submitted. It is understood that by this approval, the undersigned, do not necessarily endorse or approve any statement made, opinion expressed or conclusion drawn therein, but approve the thesis only for the purpose for which it is submitted.

Committee of final examination for evaluation of thesis:

.....

.....

Signature of Examiners

FACULTY OF ENGINEERING AND TECHNOLOGY
DEPARTMENT OF MECHANICAL ENGINEERING
JADAVPUR UNIVERSITY
KOLKATA

CERTIFICATE OF RECOMMENDATION

*We hereby recommend that the thesis presented under our supervision by **SRI Sohag Sutar**, entitled, “**DESIGN OF OPTIMISED PLATE VELOCITY CONTROLLER OF A LABORATORY SCALE ROT USING AN EHAS**” be accepted in partial fulfillment of the requirements for awarding the degree of Master of Mechanical Engineering under Department of Mechanical Engineering of Jadavpur University.*

.....
Dr. Pranibesh Mandal
Thesis Advisor
Dept. of Mechanical Engineering
Jadavpur University, Kolkata

.....
Prof. Dipankar Sanyal
Thesis Advisor
Dept. of Mechanical Engineering
Jadavpur University, Kolkata

.....
Dr. Gautam Majumdar
Professor and Head
Dept. of Mechanical Engineering
Jadavpur University, Kolkata

.....
Prof. Chiranjib Bhattacharjee
Dean of Faculty Council of
Engineering & Technology
Jadavpur University, Kolkata

ACKNOWLEDGEMENT

I would like to offer my sincere thanks to all who provided me this opportunity and granted me the capability to proceed successfully with my thesis. This thesis appears in its current form due to the assistance and guidance of several people.

I express my deep sense of gratitude to my supervisors **Dr. Pranibesh Mandal** and **Prof. Dipankar Sanyal** for their inspiration, support, academic and personal guidance throughout the course work. I'm grateful to them for being very supportive in letting me pursue my interests outside of academics, and encouraging me to learn and read widely.

It gives me great pleasure to acknowledge my ineptness to **Prof. Saikat Mookherjee** for his time to time advice and assistance during this work.

I'm very thankful to **Prof. Gautam Majumdar**, Head of Mechanical Engineering Department, Jadavpur University and **Prof. Chiranjib Bhattacharjee**, Dean Faculty Council of Engineering & Technology, Jadavpur University for their support in academic matters.

I would like to thank all faculty members and research scholars associated with Project Neptune laboratory for their valuable inputs and continued support. Special mention is owed to Nitesh Mondal, Souvik Choudhury, Prabir Biswas and Aniruddha Saha in this regard and my thanks also goes to all Fluid Mechanics and Hydraulics lab assistants for providing excellent working experience.

I also like to thank all my batch mates: Afzal Hussain, Saukrit Kumar Chandra, Sobhan Pandit and Samar Mondal for their co-operation, help and motivation. Apart from this, I am also thankful to my juniors specially Samarpan, Abhyuday and Prahar.

Last, but most importantly, I'm grateful to my parents and family for their love, blessings and support throughout this endeavor. This thesis, a fruit of the combined efforts of my family members, is dedicated to them as a token of love and gratitude.

Date:

Javavpur University,
Kolkata, 700032

Regards,
Sohag Sutar

ABSTRACT

Ultra-Fast Cooling (UFC) technique has enabled the steel industries to produce a large variety of steel grades due to its wide range of cooling rates. The laminar cooling method used in traditional hot rolling mills has been replaced by UFC to a huge extent. UFC requires a Run-Out Table (ROT) over which the cooling process is being carried out. For experimental study the long cooling bay is to be replicated by a short one, so a laboratory scale ROT of much shorter length about 1.5m is implemented to carry out the experiment of generating different cooling rates, thereby requiring reciprocating motion of the hot steel plate coming out of a furnace. Like laminar cooling, for giving the constant velocity motion to the hot billets coming out of furnace, in laboratory a reciprocating motion is given to the hot steel plate over the ROT by an Electro-Hydraulic actuation system. It is necessary to ensure the magnitude of the reciprocating velocity of the hot steel plate to be constant throughout most part over ROT, but for reciprocating motion there will be a primary acceleration and end retardation. The objective of the present work is to design such an electro-hydraulic actuation controller for giving a well sounded reciprocating motion of constant speed with minimum primary acceleration and end retardation for the hot steel plate. Starting from a feed-forward estimation to a proper feedforward modelling along with a PI controller has been successfully implemented to get more or less good matching with the sinusoidal tracking motion demand of different frequencies.

Contents

	Page No
DECLARATION OF ORIGINALITY AND COMPLIANCE OF ACADEMIC ETHICS	i
CERTIFICATE OF APPROVAL	ii
CERTIFICATE OF RECOMMENDATION	iii
ACKNOWLEDGEMENT	iv
ABSTRACT	v
LIST OF FIGURES	vi
NOMENCLATURE	viii
Chapter 1 LITERATURE REVIEW AND SCOPE OF PRESENT WORK	
1.1. Literature Review	1
1.2. Scope of present work	6
Chapter 2 SYSTEM DESCRIPTION	7
Chapter 3 MATHEMATICAL MODELLING AND EXEPERIMENTAL PROCEDURES	
3.1 Introduction	15
3.2 Mathematical Modelling	15
3.3 Experimental Procedure	17
Chapter 4 RESULT AND DISCUSSIONS	20
Chapter 5 CONCLUSION AND FUTURE SCOPE OF WORK	
5.1. Conclusions	29
5.2. Future scope of work	29
References	

LIST OF FIGURES

Figure No.	Title of the Figure	Page No.
Figure 2.1	Schematic Diagram of the Laboratory Scale Setup	7
Figure 2.2	Nozzle Bank and Cooling section	8
Figure 2.3	Picture of the Furnace	9
Figure 2.4	Schematic of the EHAS	12
Figure 2.5	Picture of The Laboratory Scale EHAS	14
Figure 3.1	Simulink Programming for the Controller	18
Figure 3.2	Circuit Diagram of the EHAS Feed-Forward control as well as PI incorporation	19
Figure 4.1	Plot of System Response for Open Loop Controller of 0.1 Hz demand	20
Figure 4.2	Plot of System Response for Open Loop Controller of 0.15 Hz demand	21
Figure 4.3	Plot of System Response for Open Loop Controller of 0.18 Hz demand	21
Figure 4.4	Plot of System Response for Open Loop Controller of 0.25 Hz demand	22
Figure 4.5	Plot of System Response for Open Loop Controller of 0.3 Hz demand	22
Figure 4.6	Plot of System Response for Open Loop Controller of 0.4 Hz demand	23
Figure 4.7	Plot of System Response for Open Loop Controller of 0.6 Hz demand	23

Figure No.	Title of the Figure	Page No.
Figure 4.8	Plot of System Response for Open Loop Controller of 1 Hz demand	24
Figure 4.9	Plot of System Response for Closed Loop Controller of 0.1 Hz demand	25
Figure 4.10	Plot of System Response for Closed Loop Controller of 0.15 Hz demand	25
Figure 4.11	Plot of System Response for Closed Loop Controller of 0.18 Hz demand	26
Figure 4.12	Plot of System Response for Closed Loop Controller of 0.25 Hz demand	26
Figure 4.13	Plot of System Response for Closed Loop Controller of 0.3 Hz demand	27
Figure 4.14	Plot of System Response for Closed Loop Controller of 0.4 Hz demand	27

NOMENCLATURE

e	Total Voltage Generating
e_{ff}	Feed-Forward Voltage
e_{fb}	Feed-Back Voltage
K_P	Proportional gain constant
K_I	Integral Gain Constant
y	Actual Actuator Displacement
y_d	Demanded Actuator displacement
y_e	Displacement Error ($y_d - y$)
y_{lvdt}	Displacement measure by LVDT
t	Time
s	Laplace Transform Variable
Q	Volume Flow Rate Entering Into the Actuator
A_1	Area of Piston at Cap end
A_2	Area of Piston at Rod End
C_{v1}	Valve coefficient for port 1
C_{v2}	Valve coefficient for port 2
W_p	Width of the port
ρ	Density of oil used for EHAS
P_1	Pressure in cylinder 1
P_2	Pressure in cylinder 2
x	Displacement of the disc in the PV

Chapter 1

Literature Review

and Scope of

Present Work

1.1. Literature Review

Steel strips and its products are widely used in many engineering applications. Different types of steel grades having different metallurgical properties are used in various industries depending upon its application. Desired Thermo-Metallurgical properties of steel can be get by providing a well-controlled cooling rate to this hot rolled steel billets. Also during heat treatment, cooling rate controls the microstructure of steel. So, cooling rate is the most important part of steel industries to produce different types of steel.

Recently UFC is a widely used cooling technique, which require a ROT over which steel is getting cooled. In ROT there is an arrangement for air cooling, water cooling or air atomised spray cooling by nozzles to generate very high cooling rate. Cooling through water jets and sprays has been a topic of discussion among researchers for a long time. Yuan et al. [1] assessed the range of overall convective heat transfer coefficient to be roughly $4\text{-}8\text{kW/m}^2\text{K}$ at a cooling rate in the range of $300\text{-}400^\circ\text{C/s}$ during ultrafast cooling of a $3\text{mm}\text{-}4\text{mm}$ thick steel plate by using finite difference method. Wang et al. [2] examined the outcome of water flow rate on the heat transfer coefficient and surface temperature with the cooling water jet flow rate varied from 0.9 to $2.1\text{m}^3/\text{h}$. Hauksson et al. [3] executed time dependent cooling of a flat, upward facing fixed steel strip. The cooling was done by a highly sub cooled free surface water jet. Finally a numerical finite difference model established to calculate the heat flux using different temperatures evaluated at the surface as well as at different points along the length of the plate. This is used to ascertain the effect of water flow rate and sub-cooling on the heat transfer. Stewart et al. [4] observed that in case of quenching through water spray of steel billets, when heated over 1000°C its heat transfer coefficient reduced sharply above the Leiden frost temperature. Xu et al. [5] drafted an iterative and sequential inverse heat transfer analysis process and used it into a 2-D finite element program. Then as a stationary hot plate is cooled by water jets on an industry scale test setup, the developed program is used to establish the heat fluxes at the stagnation points of the plate. Gradeck et al. [6] examined the effect of heat transfer by a sub-cooled jet impinged on a hot moving cylinder along a line parallel to the symmetry axis. Thermocouples were used to evaluate the time varying wall temperature and the respective wall heat fluxes were measured through an inverse conduction method. Hosain et al. [7] examined the effect of heat transfer of water jets impinging on a hot steel strip under temperatures below the boiling point to concentrate on the convection heat transfer phenomena which is a major step prior the boiling. They provide single axisymmetric jet and a

pair of interacting jets using the RANS model under steady and transient conditions as well as the $k-\varepsilon$ turbulence model considering both 2D axisymmetric and 3D simulations applying two sets of boundary conditions, constant temperature and constant heat flux at the surface of the steel plate. Hatta et al. [8] examined the cooling process of a hot moving steel plate which is cooled by a water curtain. The effect of the travelling velocity on the cooling rate was examined experimentally as well as numerically. Samanta et al. [9] provided the visualization of heat-lines and isotherms during cooling process of a hot moving steel plate. They take into account single water jet cooling and have taken initial temperature of the plate as 780°C, water jet velocity as 0.8m/s, plate velocity as 0.1m/s, plate length as 1.5m, temperature of water jet as 38°C and half plate thickness 12mm. They observed a thermally unaffected zone in the computational domain using a divider heat-line. Afterwards, the effects of water jet velocity (0.8-1.6m/s), plate velocity (0.1-0.6m/s) and heat transfer coefficient on the thermally unaffected zone and the heat transfer were anticipated in their work. Wang et al. [10] examined the heat transfer of a jet impinging on the top and bottom surface of a hot plate and studied the differences of heat flux and wetting front propagation. Wang et al. [11] employed a model using inverse heat conduction to develop a dimensional finite difference program for evaluating the local convective heat transfer coefficients and the concurrent temperature of a stationary hot steel plate under the influence of multiple top circular plates on a run out table (ROT). The experiments were accomplished under time varying ambience. Mitra et al. [12] examined the Laminar jet cooling of a heated flat steel surface and compared the boiling heat transfer behaviour of TiO₂ and MWCNT Nano fluids with that of water. It is observed that the rate of cooling is improved by employing Nano fluid jets and the shift from “film” to “transition” boiling regime takes place earlier for Nano fluid. Liu et al. [13] examined the effect of cooling water temperature, initial steel plate temperature and jet diameters on heat transfer by sprays, water jets or water curtains striking on both sides of a long continuous plate consisting of red hot steel that is rolled onto it. Nobari et al. [14] carried out experiments on a pilot scale run-out table using industrial size jets and consequently a heat transfer model was suggested for jet impingement cooling of steel plates. The suggested model mapped boiling curves according to different positions on the plate area. Lv et al. [15] carried out heat transfer analysis of free single jet impingement employing SiO₂-water Nano fluids comprising of various volume concentrations (1%, 2% and 3%). The result of the varying nanoparticles volume concentrations, the impact angle, nozzle-to-plate distance, the Reynolds number and on the heat transfer performances are

addressed. The heat transfer experiments are also investigated along the radial direction. Barman et al. [16] have performed a detailed investigation on the thermal behaviour during cooling of a steel plate that is cooled by multiple jets of pressurized water from two sides. They took into account a system of 10 equally spaced water jets for each of the two plate surfaces and presumed the initial plate temperature and the water jet temperature to be 775°C and 35°C respectively with a plate thickness of 20mm. They reckoned an effective heat transfer coefficient to describe the jet and the surface interaction and discretized the main equation on the basis of finite-volume method using a power-law strategy and resolved that with the help of TDMA algorithm. They anticipated the distribution of temperature within the strip and examined the effect of plate velocity on the temperature distribution and associated cooling rate. Lyons et al. [17] examined the effect of varying water droplet size on the heat transfer properties of an air jet impinging on a heated plate. Kuraan et al. [18] examined the effect of nozzle to strip distance for a free water jet striking on a flat surface. The effect of nozzle-to-plate distance on a free water striking jet was examined and the effect on stagnation pressure, Nusselt number, and hydraulic jump diameter which finally reflected the same trend at low nozzle-to-plate distance.

In the current experiment, a Laboratory scale ROT with a furnace and nozzle bank set-up along with compressor and electro-hydraulic power pack has been implemented for more detail analysis of spray cooling. In the cooling zone, the industrial system has a provision of giving unidirectional linear motion to the sheet metal between a hot rolling mill and a coiler. However, it is difficult to achieve such a long system in the laboratory scale process line. So, a reciprocating motion is given to the heated MS plate so that experimental analysis can be carried out on a unit of much smaller length. For this purpose, an Electro-Hydraulic Control System has been proposed. The major challenge of the electro-hydraulic actuation system is to accomplish a quick velocity reversal, to simulate the constant speed motion of the sheet in industrial line and to ensure minimum time lag between primary acceleration and end retardation of the plate at the beginning and end of each stroke. Electro-hydraulic systems and their control have been a topic of discussion for scientists for a long time. Electro-hydraulic systems and their control have been a topic of discussion for scientists for a long time. Mandal et al. [19] employed a bacterial foraging optimization, or BFO, along with a simple swarming method to design a real-time controller of an electrohydraulic system. The flow-related continuous nonlinearities were balanced with a fuzzy voltage and a

feedforward voltage was used to serve for known external loading and discontinuous internal nonlinearities due to the valve dead-band and cylinder stiction. Tafazoli et al. [20] investigated and measured friction and compensated for its effects in the control of an electrohydraulic manipulator. For enhancing the tracking performance of the manipulator, a novel observer-based friction compensating control method is developed which is based on acceleration feedback control. The experimental outcome showed that this controller substantially enhances over a conventional PD controller. Habibi et al. [21] connected the system requirements to design parameters for an Electro Hydraulic Actuator (EHA). Considering the mathematical model of EHA is done and then this result is employed to connect its performance to its design parameters through an array of mathematical functions. The experimental and theoretical performances of the prototype are compared to authenticate the proposed mathematical functions and a much enhanced design is put forward. Sarkar et al. [22] employed a feedforward controller model on a rugged electrohydraulic system with a similar proportional valve and a cylinder. But here a PID feedback of the piston displacement was applied for absorbing the un-modelled effects like the large bandwidth, low deadband and flow nonlinearities in proportional valves and highly nonlinear friction in the cylinders. A real-coded genetic algorithm (RCGA) is used to analyse all the control parameters. Guo et al. [23] provided a nonlinear cascade controller based on an extended nonlinearity observer which in the existence of external nonlinearity as well as parameter uncertainties was used to track desired position trajectory of EHAS. The external perturbations and parameter uncertainties were separately taken care of by the given extended disturbance observer. Lyapunov theory was used to check the stability of the overall system. The result showed that the combination of the nonlinear cascade controller and the extended disturbance observer presented excellent tracking performance in spite of the uncertainties and nonlinearities. Zhang et al. [24] designed a suitable control algorithm for an electrohydraulic steering system and also took into consideration for the non-linear compensation of the electrohydraulic valve. He calculated the test results employing different control algorithms and a non-linear compensation algorithm on a John Deere 8200 tractor and finally based on the evaluation results designed the required control algorithm. Kim et al. [25] suggested an adaptive back-stepping control (ABSC) method to overcome the problem of system nonlinearities of EHAS successfully and to enhance their tracking performance. Here, the system nonlinearities in EHAS are reviewed as only one term and to obtain the implicit controls for stabilizing the closed-loop system, the Lyapunov control function (LCF)

is used as the current rule for the system nonlinearities term. Ho et al. [26] examined a unique hydraulic energy-regenerative from its modelling phase to its final control stage. Simulation and experiments were executed to calculate the validity of the used mathematical model and the effectiveness of the control system. The outcome showed that the system was operative and that the round trip recovery efficiency varied from 22% to 59% for the test specimen. Alleyne et al. [27] employed a precise model of an electro- hydraulic system to develop its force tracking controller which is based on a Lyapunov control algorithm. The Lyapunov based parameter adaptation was employed to account for the system parameter nonlinearities. An experimental valve-controlled cylinder is taken on which the combined control law and the adaptation technique are applied upon. Qiu et al. [28] employed a feedforward-plus-proportional-integral-derivative (FPID) controller for enhancing the control performance of the electrohydraulic steering system of an off-road vehicle. In the feedforward-plus-proportional-integral-derivative controller, an inverse valve transform is applied in the feedforward loop to compensate for an electrohydraulic steering system deadband and a conventional PID feedback loop is utilised to minimize the tracking error in steering control. Watton et al. [29] examined hydraulic actuation systems with different aspects and a linearized model is provided by him with two sets of coefficients for retraction and extraction conditions respectively and both set is depicted by taking actuator area ratio as parameter. Chinniah et al. [30] identify flaws in EHA systems by utilizing a strong extended Kalman filter, which is utilized to calculate viscous friction and effective bulk modulus. Watton et al. [31] determined that as area ratio increases, stability margin accentuates and drove home the fact that it is the actuator position on which the actuator gain at instability is based on. Similarly, Wang et al. [32] utilised a sliding mode controller in a highly accurate electrohydraulic actuator (EHA) system with non-linear discontinuous friction effects. A linear quadratic approach for delimiting the discrete-time sliding surface for non-linear systems is utilized in this study. Also, Kaddissi et al. [33] utilised a robust indirect adaptive back-stepping control (ABSC) scheme to electrohydraulic actuation systems having changes of viscous friction coefficient and effective bulk modulus due to temperature variations. Taylor et al. [34] established a state dependent parameter (SDP) control system which is optimized from experimental data to control the hydraulically actuated manipulators of a nuclear decommissioning robot. The SDP is a time varying voltage signal which depicted a time-varying gain. This model gave more precise determined motion in comparison to a constant gain one. Jun et al. [35] submitted a self-tuning

PID controller using fuzzy logic to control the BLDC motor of an EHAS which has some non-linear characteristics such as the saturation of motor power and dead-zone owing to static friction. Mandal et al. [36] established a fuzzy-feedforward-bias controller and employed a genetic code to optimize the controller parameters of an electrohydraulic system consisting a proportional valve and industry-grade cylinder which is to be utilised in heavy duty applications and ultimately the real-time control experiments showed excellent tracking throughout the cycle for sinusoidal displacements beyond 1.5 Hz.

The above review shows that significant work has been done in the area of jet and spray impingement cooling of steel plates, although there is a necessity for further studies on UFC of moving steel plates. The set up used for the current study is that of a laboratory scale ROT where the constant velocity motion of steel billet in actual ROT is replaced by reciprocating motion of heated Mild steel (MS) plate due to space constraints. The real-time reciprocating motion tracking control is done using a low-cost industry grade EHAS for a number of sinusoidal motion control demands using a feedforward-feedback controller. The mathematical model for the highly nonlinear actuation system has also been developed that is necessary for development of the feedforward controller. Overall nice tracking control has been achieved for a number of control demands.

1.2. Scope of present work

The main objective of the present work is to design a Feedforward-Feedback controller for the Electro-Hydraulic Actuation System (EHAS) so that the actuator rod movement traces a sinusoidal displacement profile and that at a near constant velocity. Within the scope of the present work the following objectives are aimed towards:

- Finding out all the mathematical relations for the system.
- Performance analysis through modelling and simulation of the actuation system in MATLAB-Simulink for both plant and the controller.
- Making a Feedforward estimation for the EHAS.
- Making the proper Feed-Forward modelling in LabVIEW for the EHAS.
- Check for optimum plate velocity by Precisely choosing the Parameters/Constants for the EHAS
- Run the EHAS by Feed-Forward modelling along with a PI Feed-back controller for smooth running of the actuator.

Chapter 2

System Description

The schematic diagram of the set-up is shown in the figure 2.1. The whole set-up has different section, such as heating section consists of a furnace, cooling section consists of a ROT and bank of nozzles, mechanical handling section, controlling section comes up with an electrohydraulic power pack, apart from that there is a compressor and several accessories.

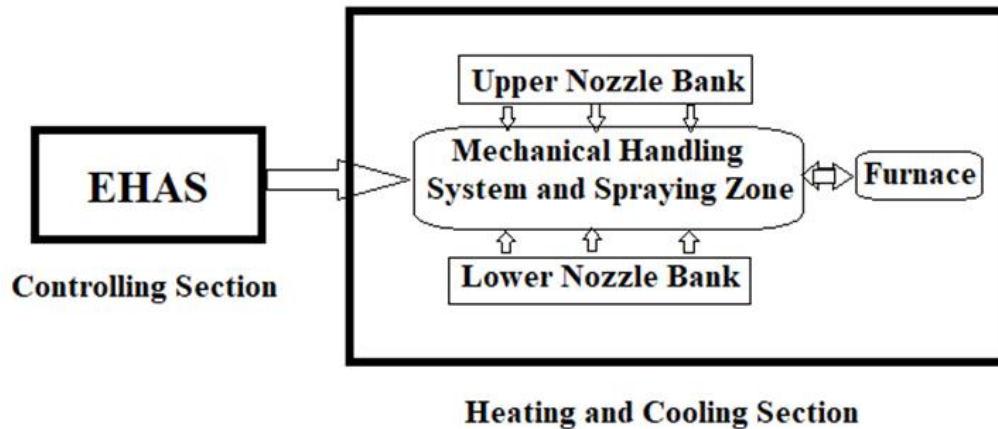


Figure 2.1 Schematic diagram of the laboratory scale set-up

Steel plate first placed over the inner tray and this tray goes inside the furnace. Then in the furnace the plate is heated to a predefined temperature. After heating the plate along with the inner tray, manually we remove the plate from the furnace and put it over the outer tray so that it can be attached with the actuation system for cooling over ROT. Air atomised spray is provided over the plate by the upper and lower nozzle bank. There is six thermocouples connected with the plate at six different points to measure the temperature of the plate over time.

Two **nozzle banks**, each consisting of twenty nozzle units, are on the both sides of the cooling bay is used in our laboratory. There were two types of nozzle bank used in the experiment. Maker of the nozzle bank is Lechler (India) Pvt. Ltd. In our setup Full Cone Hydraulic type nozzle (nozzle no-460.366.CA) can provide maximum flow rate of 0.7 Lpm per nozzle and Air Mist type Nozzle (nozzle no- 1PM.021.30.40.00.1) can provide maximum flow rate of 5.8 Lpm per nozzle. From figure 2.2 it can be seen that there are two rows of hydraulic nozzles, five in each row on both sides of the plate which makes it a total of twenty of them, also how the thermocouples were connected with the test plate also shown in the figure 2.2



Figure 2.2 Nozzle Bank and cooling section

In our laboratory we have a furnace where we can heat our test plate up to 1200⁰C and the rating power of the furnace is 21 KW. Maker of the furnace is Kanthal, Sandvik Asia Ltd (serial no. - SF-074). The depth, width and height of the working chamber is 800mm, 800mm and 300mm respectively. Power supply needed for the furnace is 415 V , 50 Hz, and 3 Phase AC supply. The maker of the temperature controller is Eurotherm (model no.-2416). As shown in Figure 2.3 the furnace door operation is vertical lifting type and manual.

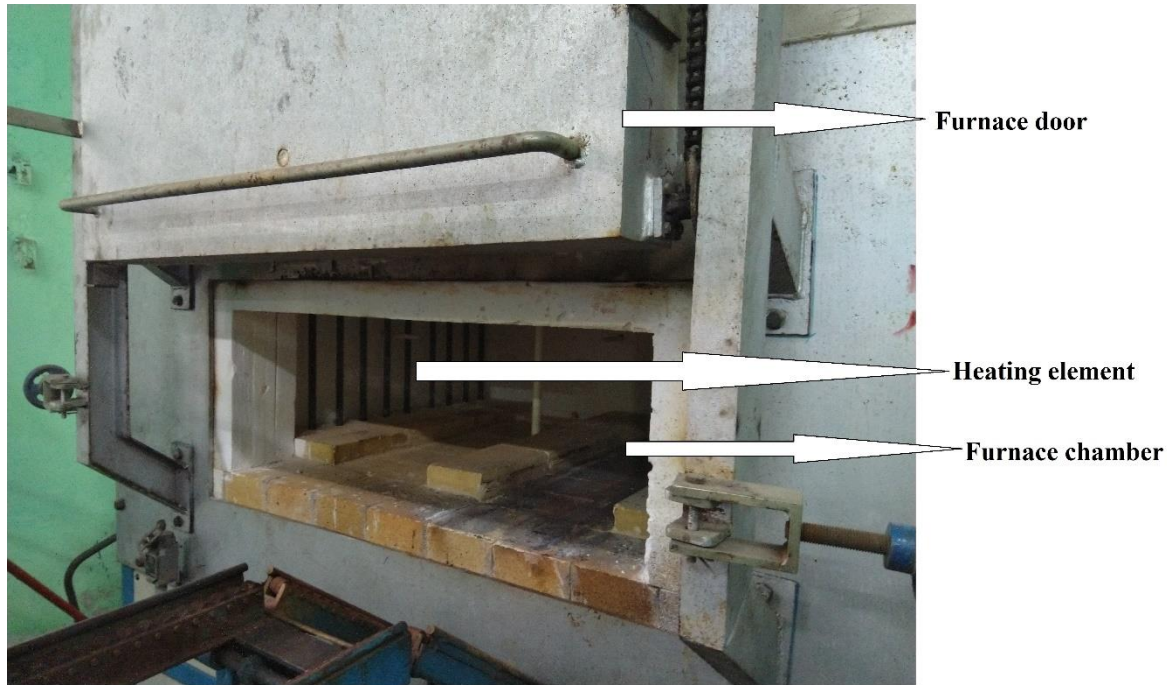


Figure 2.3 Picture of the furnace

The details of the **airline component** associated with the experiment is given below-

1. **Compressor:** Maker of the compressor is FLGI equipment Ltd. (Model TS 05 120 H). The maximum working pressure of the compressor is 12 kgf/cm^2 , it runs at 1450 rpm (Unit rpm is 925) and 50 Hz. Power rating of the compressor is 5.5 hp, and air receiving capacity is 220 L.
2. **Ball Valve (BV):** Maker of the ball valve is mevada Engineering Works (P) Ltd. (model no. - BL-30 F-W-A3). Size rating of the BV is 1" S.W.
3. **Air Filter:** The maker of the Air Filter is Shavo Norgan (model no.-SF-17-800 M8- DC). It can hold maximum inlet pressure of 17.5 kgf/cm^2 and size is 1" BSP (F)
4. **Pressure Gauge:** Maker of the Pressure gauge is Wika (Model No. - EN837-1). The range the pressure gauge is 0 to 10 bar and size is $\frac{1}{2}$ " BSP (M).

5. **Needle valve:** Maker of the Needle Valve is Expo Engineering Ltd. (Model no- EN 837-1). Size and Rating of the NV is ½" BSP (F).
6. **Solenoid Valve:** Maker of the solenoid valve is Avcon (Model No-9160K25/CI/S4/BN-A1). Size and rating of the SV used is 1" FLGD, and gives supply of 24V.
7. **Glove Valve:** There was two glove valve. Maker of the glove valve is Mevada Engineering works Ltd. (Model No. - GB-1-R-W-A4). Size and Rating: 1", S.W., and Size and Rating: ¾", S.W.

The details of the **waterline components** which has been used in the experiment is given below-

1. **Water Filter:** Two water filters have been used. Maker of the water filter is Filtration Engineers India Pvt. Ltd.
Filter 1- Model No- FR-244450NB, Size is 2", Mesh of 200µ, Maximum operating Pressure of 5 bar.
Filter 2- Model No- FR-244440NB, Size is ½" with Mesh of 100µ. Maximum operating Pressure is 5 bar.
2. **Ball Valve:** Three ball valves have been used in in the set up. Maker of the ball valve is mevada Engineering Works (Model No. - BL-30-F-W-A3). Size of two ball valve is 2" and other one have ½".
3. **Pump:** Maker of the pump is Grundfos (Model No. - CR10-4-A-FJ-A-E-HQQE). It has maximum flow rate of 10 M³/hr, and shut off head of 40.8m. Operating speed is 2890-2910rpm.
4. **Glove Valve:** There were seven glove valves in the set up. Maker of the glove valve is Mevada Engineering works Ltd. (Model No.- GB-1-R-W-A4)
Glove valve 1-4: Size: 1", S.W
Glove valves 5: Size: 1 ½", S.W
Glove valves 6-7: Size: ½", S.W
5. **Pressure Gauge:** Three pressure gauges have been used in in the set up. Maker of the Pressure Gauge is Wika (Model No. - EN837-1).These are ½", BSP (M) and have an operating range of 0-10 bar.
6. **Solenoid Valve:** Three solenoid valves have been used in in the set up. Maker of the solenoid valve is Avcon

Solenoid valve 1: Model no.-9162K25/CI/S4/BN/A1, Size 1", FLGD, 150, Supply: 24V DC

Solenoid valve 2: Model no. - 9160K25/C1/S4/BN/A1, Size: 1", FLGD, 150, Supply: 24V DC

Solenoid valve 3: Model no. - 9160K35/C1/S4/BN/A1, Size 1 ½", FLGD, 150#, Supply: 24V DC

- 7. Electromagnetic Flow Meter:** There were two electromagnetic flow meter in the set up. Maker of the electromagnetic flow meter is Endress and Hauser (Model No. PROMAG 10P).

Electromagnetic flow meter 1: Size: 1", FLGD, Maximum Flow: 10m³/h, Maximum Pressure: 10bar, Supply: 220V AC, 50Hz.

Electromagnetic flow meter 2: Size: 1 ½", FLGD, Maximum Flow: 10m³/h, Maximum Pressure: 10bar, Supply: 220V AC, 50Hz

- 8. Needle Valve:** Three pressure needle valves have been used in in the set up. Maker of the Needle Valve is Expo Engineering Ltd. (Model no. - E8-NVFN) and the size is ½", BSP (F)

In steel industries continuous cooling is used but in the laboratory due to space constraints and for experimental purpose a reciprocating motion is provided to the plate by an **Electro Hydraulic Actuation System** (EHAS). The EHAS consists of an actuator, a proportional directional valve, pump, and motor and pressure valves. The schematic diagram of EHAS is shown Figure 2.4.

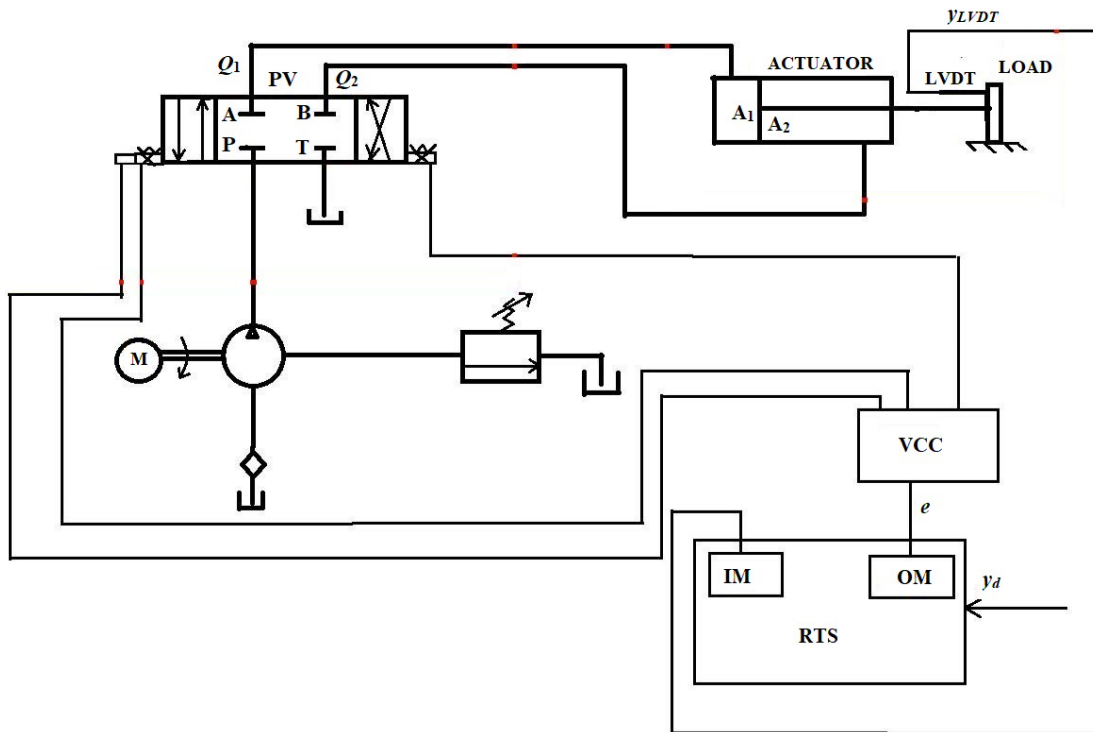


Figure 2.4 Schematic of the EHAS

From figure 2.5 it is visible that in our proportional valve we have two unmetered ports P, T and two metered ports A, B. Through P port high pressure oil from the pump enters into the Proportional Valve (PV) and T port drives out oil from the PV to the tank at low pressure near about three times of atmospheric pressure. Ports P and T remain open throughout the course of operation. Ports A and B connect the lines between the two ends of the actuator cylinder.

The force to impart the spool motion in the PV is realized by the solenoids, when it receives the amplified voltage from a valve control card VCC interfacing with the Real time system RTS. There is a PC interfaced with FPGA platform of the RTS through an Ethernet cable. The controller is designed and available on the LABview software installed in this PC. The RTS has an input module IM and output module OM. While the OM sends the control voltage to the VCC, the IM receives the LVDT signal corresponding to the measured displacement y_{LVDT} . The RTS is fed with a sinusoidal demand y_d .

The details of the **Electro Hydraulic Actuation System** associated with the experiment is given below:

1. Pump

A pump (Make: Rexroth, Model No. - A10VSO 45DR31R- PPAI2NOO) has been used for current experimental study. The nominal pressure of the pump is 280 Bar. The pumping capacity of the pump is liter per minute. The motor associated with the pump was ABB made. The rating of the pump was 30 Kw, 59 Hz and 1470 rpm.

2. Pressure Reducing Valve (PRV)

The pressure reducing valve is made by Yuken. The model number of the pump is EBG-03-H-11. The maximum allowable pressure of the pump is 245 Bar.

3. Oil filter

Oil filter utilized in this study is made of Hydac. The model number of the oil filter is DFBN/HC110G10B1.1. The working range of oil filter is 420 Bar.

4. PV (write full form)

The pressure reducing valve is made by Rexroth. The model number of the oil filter is 4WRE 10 E1-50- 21/G24K4/V. The flow capacity of the pump is 50 liter per minute. This pump gives supply at 24 volt DC with a dead band of $\pm 1.5V$. Solenoid resistance and input current to the solenoid are 4.1Ω and 2.6A respectively.

5. Linear variable differential transformer

The linear variable differential transformer (LVDT) is a significant element of experimental set up. LVDT utilized in this experiments is made by Gefran. Model number of LVDT is LT-M-0200S- XL02020000X000X00. The LDVT can be specified as Stroke Length: 200 mm, Linearity: $\pm 0.05\%$, Repeatability: 0.01 mm

6. Actuator

A single acting actuator is used for in the present study. The stroke length of the actuator is 200 mm and bore is of 50 mm.

7. Real time serial processor

A real time serial processor (Make: National Instruments, Model Number: NI-cRIO-9215) for experimental analysis. The sampling rate of the processor is 16 bit, 1 kHz with an accuracy of ± 100 ppm (max).

8. Input module

Two input module has been used in the current study. Both the Input modules are made by National instruments. The model number of these module are NI-cRIO-9215 and NI-cRIO-9211. The specifications of input modulator can be written as ‘4-Ch $\pm 10V$ 16 bit simultaneous analog input Max. Gain Error: 0.2%’.

9. Output Module

An output module, made by National Instruments (Model No. - NI-cRIO-9263) utilized for present study. Other specifications of output modulator are 4-Ch $\pm 10V$ 16 bit analog output Max Gain Error: 0.35%.

The picture of the above described laboratory scale EHAS setup is shown in the figure 2.5.

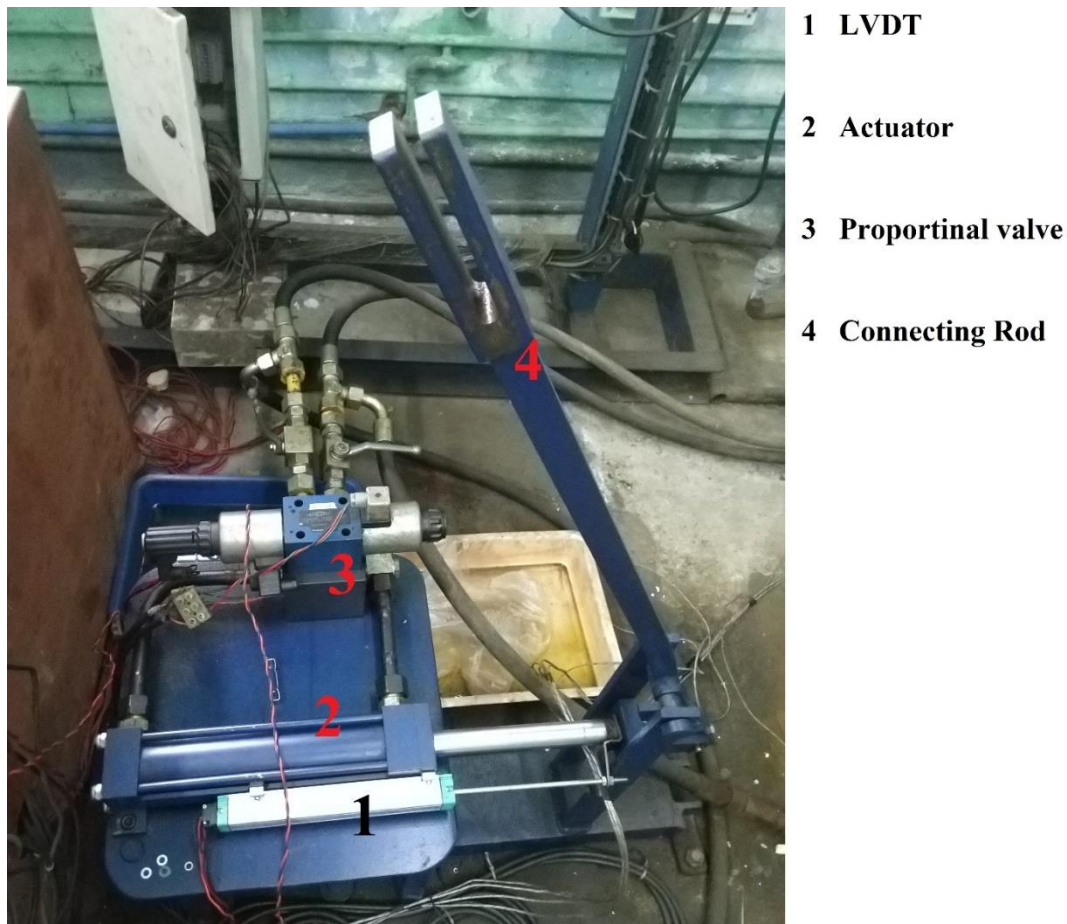


Figure 2.5 Picture of The Laboratory scale EHAS

Chapter 3

Mathematical Modelling and Experimental Procedure

3.1. Introduction

Initially a Feedforward Simulink model of the Plant was done for the EHAS present in the laboratory by taking care only mathematical equations associated with the electrohydraulic control system. In the Plant model, a voltage of sinusoidal nature for the PV was given as input and the output was displacement profile of the actuator. The nature of output from the Simulink plant model was observed for a range of input and then accordingly a controller model was framed in LabVIEW.

3.2. Mathematical Modelling

a) For extension stroke:

The flow rate (Q_1) coming out from the PV as shown in figure 2.4 is given by

$$Q_1 = C_{v1} \times W_p \times x \times \sqrt{\frac{(P_p - P_1)}{\rho}} \quad (1)$$

where P_p , P_1 , C_{v1} , W_p , x and ρ denotes pump pressure, Pressure at the cap end of the actuator, valve constant of port 1, width of the port, spool displacement of the PV and density of the oil used in the actuator respectively.

In terms of response, Proportional Valve dynamics is considered to be many times faster than motor dynamics. So, the spool displacement can be given by

$$x = K_v \times (e - e_0) \quad (2)$$

Where K_v , e are e_0 are valve coefficient, voltage at the valve end, and dead band voltage respectively. The valve being a low-cost proportional valve the deadband voltage e_0 is significantly high and required to be considered in the modelling.

Now \dot{y} being the actuator velocity, for $e \geq e_0$, the extension velocity can be given by,

$$\dot{y} = \frac{Q_1}{A_1} = \frac{Q_2}{A_2} \quad (3)$$

Where A_1 is cap end area and A_2 is rod end area of the actuator.

$$\text{So, rearranging equations (1), (2) and (3) we get } P_1 = P_p - \left\{ \frac{A_1 \times \dot{y}}{C_1 \times (e - e_0)} \right\}^2 \quad (4)$$

Where C_1 is taken as constants and are given by,

$$C_1 = C_{v1} \times W_p \times K_v \times \sqrt{\frac{1}{\rho}} \quad (5)$$

In a similar fashion, flow rate Q_2 coming out from actuator and going to reservoir through PV is given by,

$$Q_2 = C_{v2} \times W_p \times x \times \sqrt{\frac{(P_2 - P_T)}{\rho}} \quad (6)$$

Where C_{v2} , P_2 and P_T are the valve constant of port 2, pressure at the rod end of the actuator and tank pressure respectively.

$$\text{And rearranging equations (1), (2) and (6) we get, } P_2 = P_T + \left\{ \frac{A_2 \times \dot{y}}{C_2 \times (e - e_0)} \right\}^2 \quad (7)$$

Where C_2 is taken as constants and are given by,

$$C_2 = C_{v2} \times W_p \times K_v \times \sqrt{\frac{1}{\rho}} \quad (8)$$

The overall Actuator Dynamics is given considering the force balance on the actuator piston as:

$$m\ddot{y} + c\dot{y} + ky = A_1 \times P_1 - A_2 \times P_2 \quad (9)$$

Where m , k , c are the mass associated with actuator, the spring constant and the damping coefficient respectively.

Rearrangement of equations (4), (7) and (9) gives the Actuator Dynamics for extension stroke as

$$m\ddot{y} + c\dot{y} + ky = A_1 \times \left[P_p - \left\{ \frac{A_1 \times \dot{y}}{C_1 \times (e - e_0)} \right\}^2 \right] - A_2 \times \left[P_T + \left\{ \frac{A_2 \times \dot{y}}{C_2 \times (e - e_0)} \right\}^2 \right] \quad (10)$$

a) For retraction stroke:

Flow rate (Q_1) coming out from the PV as shown in figure 2.4 is

$$Q_1 = C_{v2} \times W_p \times x \times \sqrt{\frac{(P_p - P_2)}{\rho}} \quad (11)$$

By rearranging equations (2), (3) and (11),

$$P_2 = P_p - \left\{ \frac{A_2 \times \dot{y}}{C_2 \times (e + e_0)} \right\}^2 \quad (12)$$

$$\text{Similarly, } P_1 = P_T + \left\{ \frac{A_1 \times \dot{y}}{C_1 \times (e + e_0)} \right\}^2 \quad (13)$$

Rearrangement of equations (9), (12) and (13) gives the Actuator Dynamics for retraction stroke as

$$m\ddot{y} + c\dot{y} + ky = A_2 \times \left[P_p - \left\{ \frac{A_2 \times \dot{y}}{C_2 \times (e + e_0)} \right\}^2 \right] - A_1 \times \left[P_T + \left\{ \frac{A_1 \times \dot{y}}{C_1 \times (e + e_0)} \right\}^2 \right] \quad (14)$$

Equations (10) and (14) become the main governing equations for the overall system. The equations readily show the system to be a highly nonlinear one. For the setup the values of the constants are known and given as,

$$A_1 = 0.0019 \text{ m}^2, A_2 = 0.0012 \text{ m}^2, P_p = 100 \text{ bar}, P_T = 3 \text{ bar}, m = 4.5 \text{ kg}, c = 0.7 \text{ Nsm}^{-1} \text{ and } k = 39000 \text{ Nm}^{-1}.$$

3.3 Experimental Procedure

As discussed in Chapter 2, the basic setup for running the actuator consists of a positive displacement pump delivering hydraulic oil through a reservoir to the actuator via a 4-way Directional Control Valve (DCV). The solenoid of the DCV is controlled using LabVIEW on the computer. The demand signal is fed to the solenoid in the form of voltage, and the solenoid operates the DCV accordingly. Thus, our control input is the voltage given to the solenoid according to the demand. In this way, the flow of hydraulic oil to the actuator is controlled by the DCV and the actuator responds accordingly. Different frequencies of demand could be given to the actuator using LabVIEW, but before going for the laboratory experiment a MATLAB Simulink program of the **feedforward** controller was designed first. Then the variation of the output profile was observed by changing amplitude and the frequency of the sinusoidal displacement input, and then the optimum values of the unknown parameters were taken for developing the controller in LabVIEW. The Simulink Program is shown in the figure 3.1

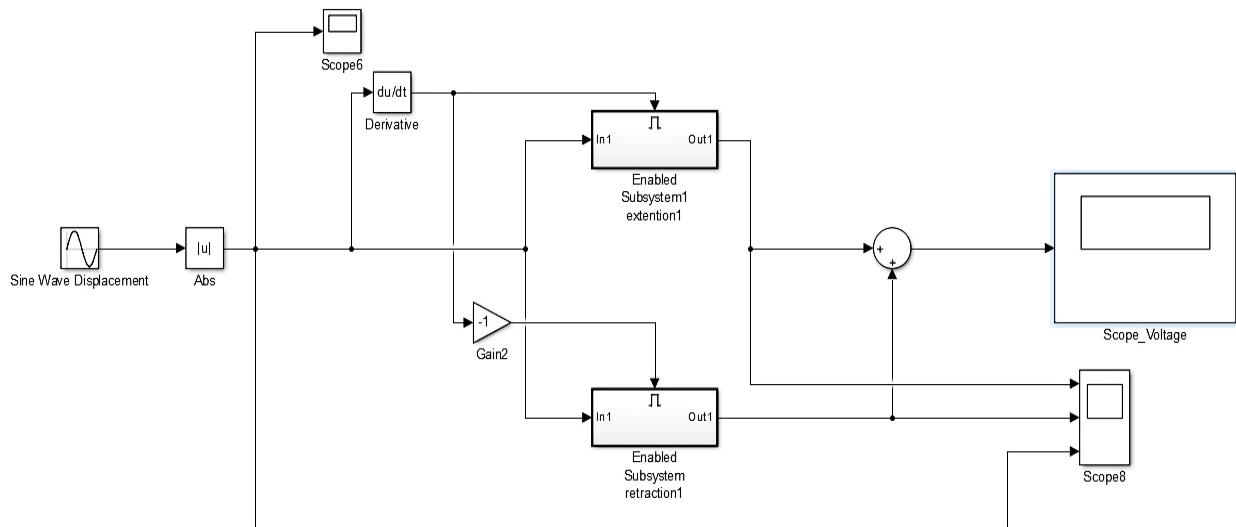


Figure 3.1 Simulink program for the Controller

So, accordingly the **feedforward** controller is designed in LabVIEW and the results were noted down for different set of input velocity of the actuator rod. In this feedforward controller demanded input was a sinusoidal displacement profile for the actuator and the corresponding voltage generated from the mathematical modelling is being feed to the PV to supply proper flow, so that actuator can trace the demanded displacement profile. In due course of the experiment again by changing the unknown parameters, variation of the output profile was examined, and the best set of parameters was selected for that setup, and then frequency of the demand was varied and it was observed that the real time system generate better result for the frequency range from 0.1 Hz to 0.25 Hz.

Next job was to **incorporation of feedback** with the feedforward modelling so that it can generate more accurate voltage to trace the demand smoothly. How we use the feedback (PI) control along with the feedforward model is shown in the figure 3.2.

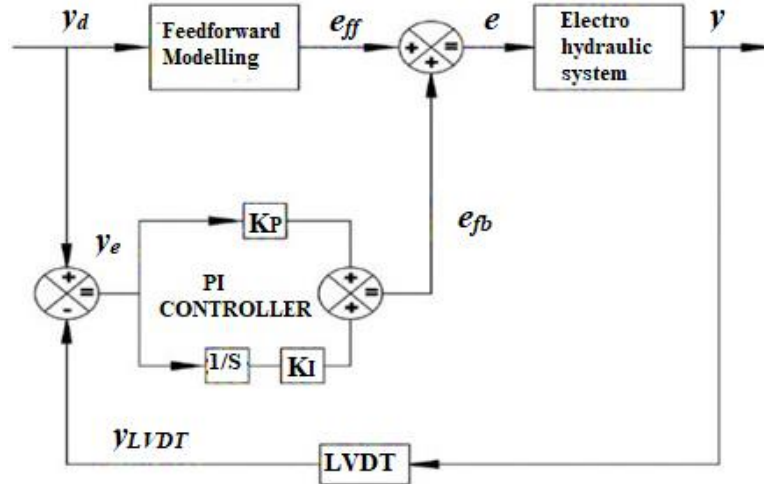


Figure 3.2 Circuit Diagram of the EHAS with feedforward control as well as PI incorporation

The LVDT fixed with the actuator is used to measure the response of the actuator against the demand. The displacement of the LVDT is assumed to be equal to the real actuator displacement, and is also utilized for generating the feedback voltage using the PI controller. The LVDT displacement is recorded in LabVIEW and again it used for studying response of the actuator for different demands from feedforward-feedback model.

Chapter 4

Results

And

Discussions

Initially only **Feedforward controller** was used at different frequency of demand displacement. The result from the feedforward controller at 0.1 Hz input frequency is shown in figure 4.1.

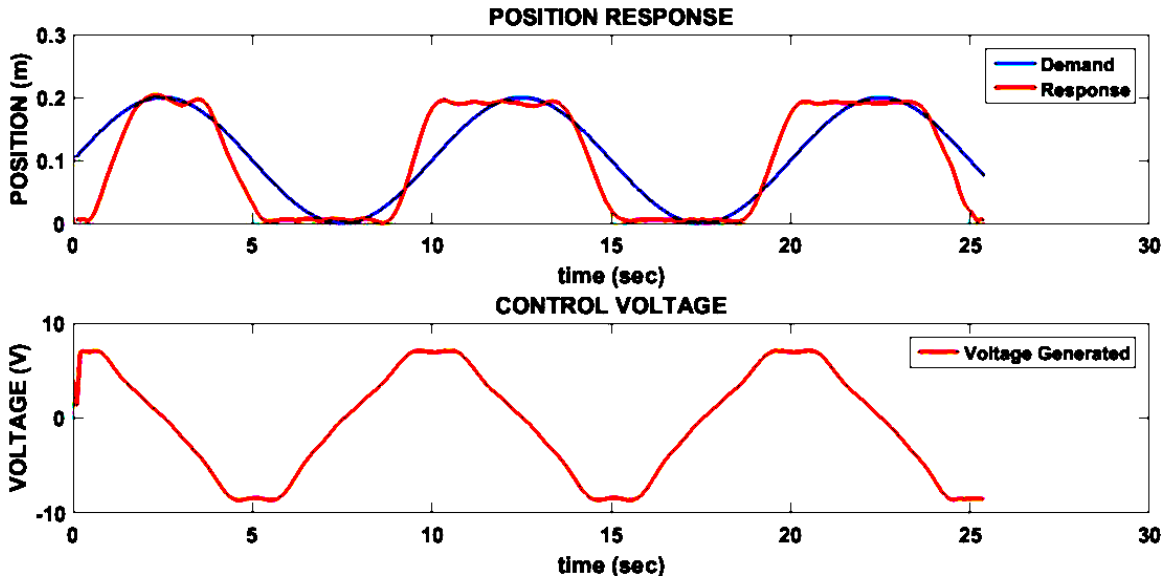


Figure 4.1 Plot of System Response for Open Loop Controller of 0.1 Hz demand

It is clear from the figure 4.1 that true actuator position response deviates from the demanded position pattern. Then a set of experiment was done by varying the frequency and it was noticed that the set-up gives better results for frequency 0.15 Hz to 0.18 Hz for the feedforward model. The results from feedforward controller at 0.15 Hz, 0.18 Hz, 0.25 Hz, 0.3 Hz, 0.4 Hz, 0.6 Hz and 1 Hz of input frequency are shown in figure 4.2, figure 4.3, figure 4.4, figure 4.5, figure 4.6, figure 4.7 and figure 4.8 respectively.

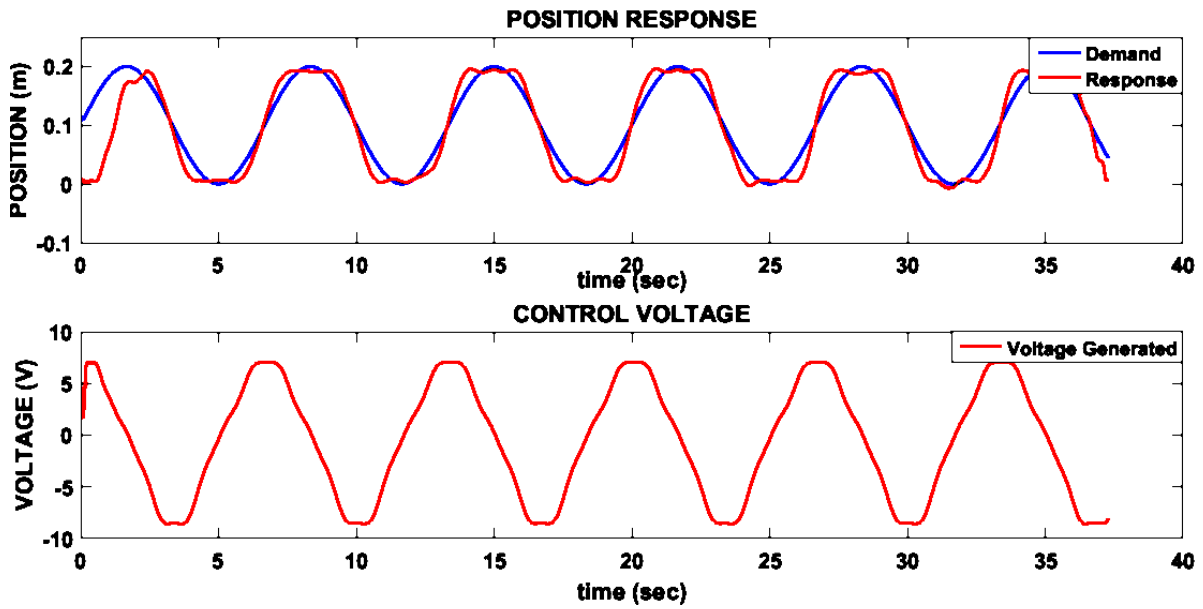


Figure 4.2 Plot of System Response for Open Loop Controller of 0.15 Hz demand

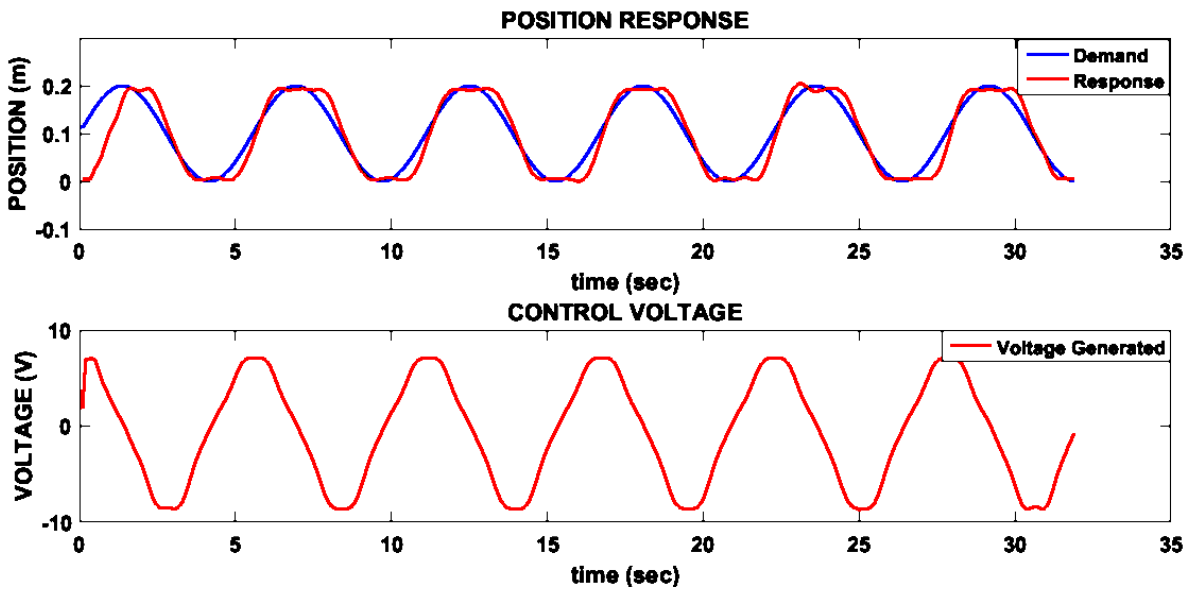


Figure 4.3 Plot of System Response for Open Loop Controller of 0.18 Hz demand

It can be seen from the figure 4.2 and figure 4.3 that the displacement error is very less and the deviation of actual response from demanded response was observed during the starting and ending of the stroke. But in spite of this, we can consider our actual displacement and demand to almost follow each other.

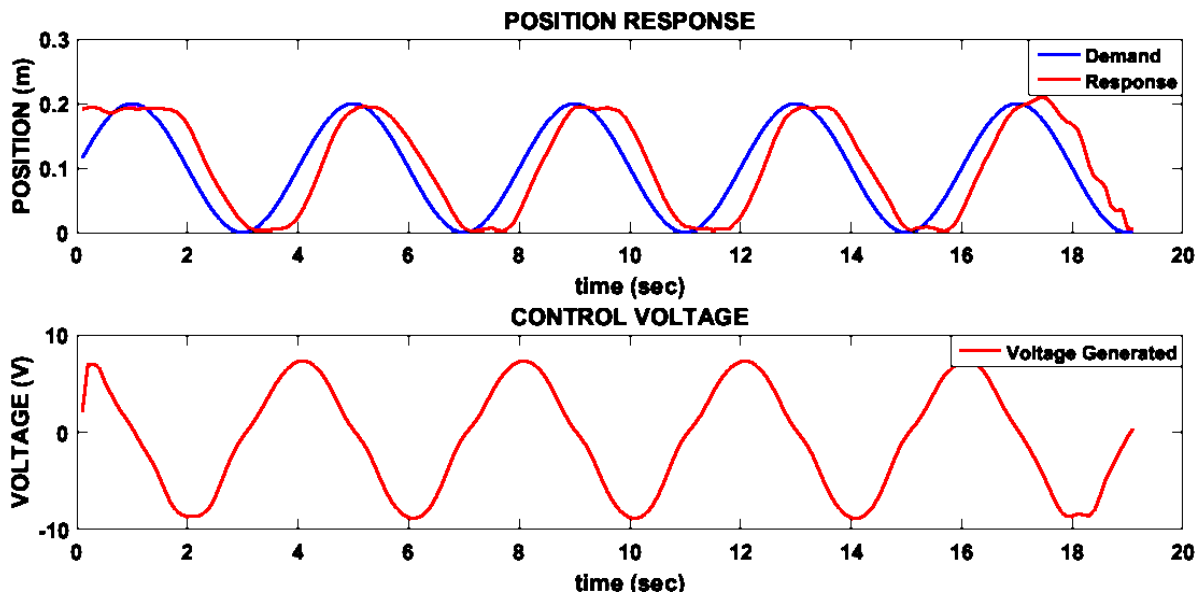


Figure 4.4 Plot of System Response for Open Loop Controller of 0.25 Hz demand

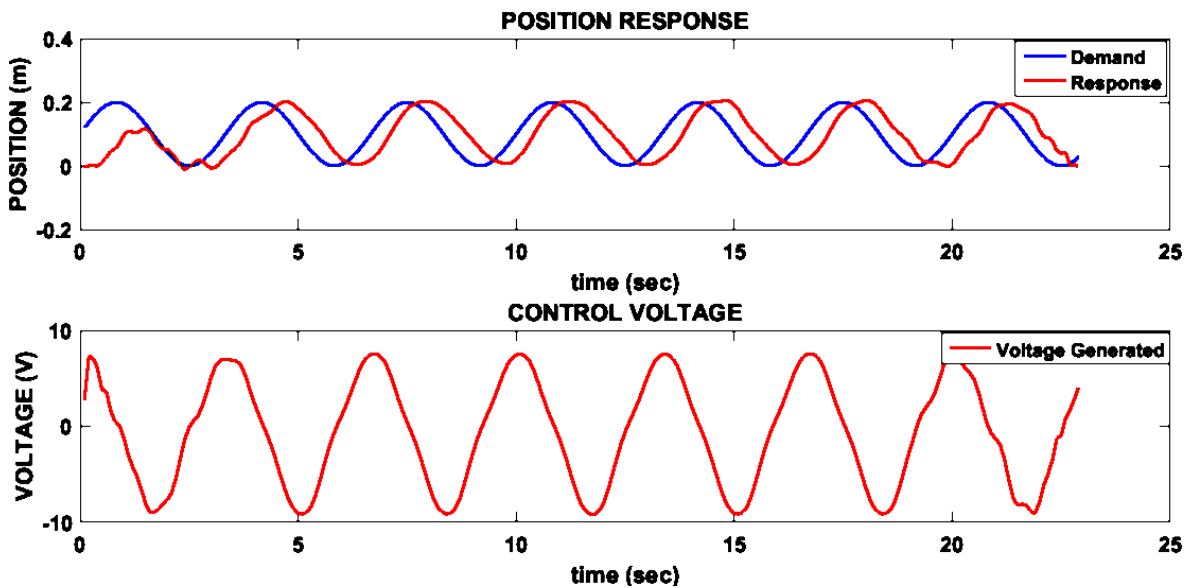


Figure 4.5 Plot of System Response for Open Loop Controller of 0.3 Hz demand

It is clear from the figure 4.4 and figure 4.5 that true actuator position response deviates from the demanded position pattern as increase of input frequency and the error in the band of

almost +15% to -15%. The velocities in both these cases are higher than that of figure 4.3. Thus a trend is observed where the error increases with the velocity demanded.

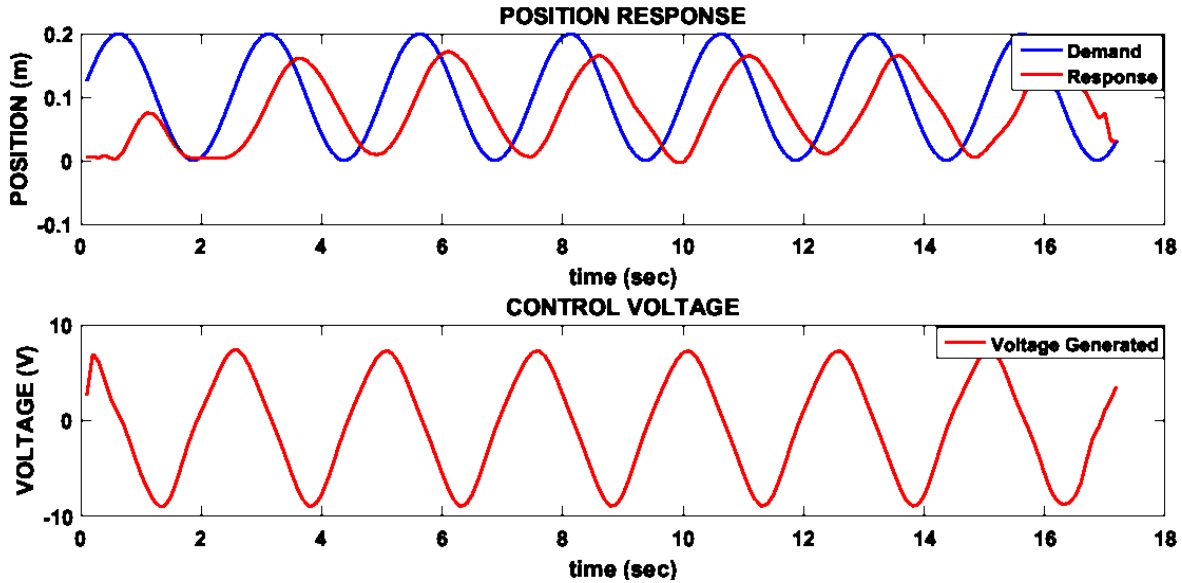


Figure 4.6 Plot of System Response for Open Loop Controller of 0.4 Hz demand

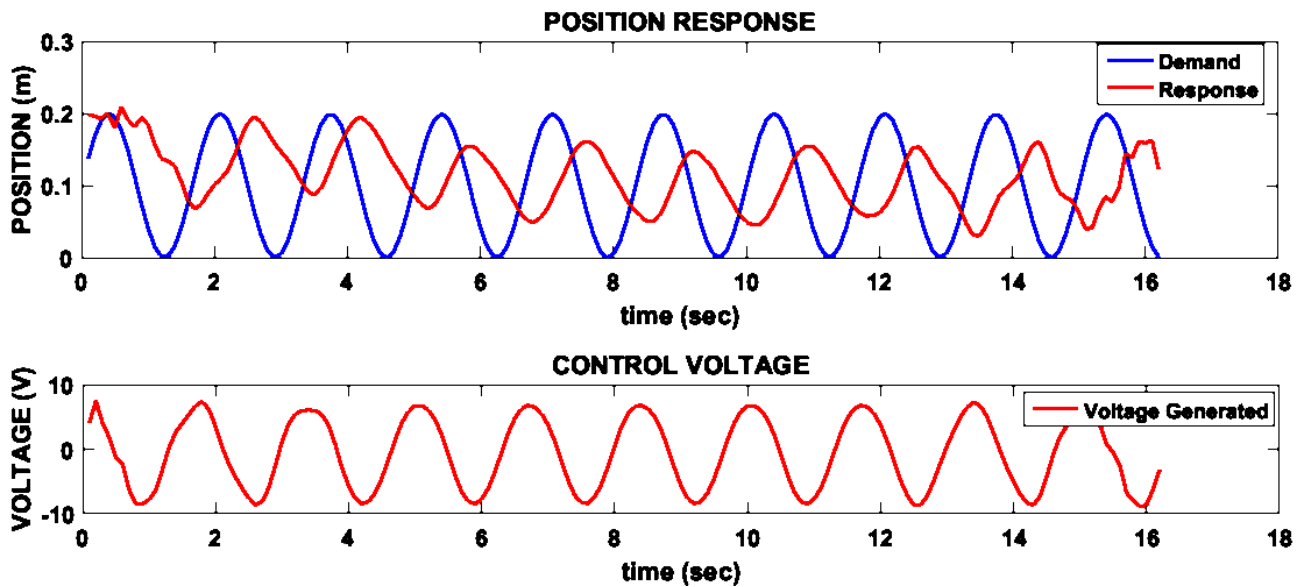


Figure 4.7 Plot of System Response for Open Loop Controller of 0.6 Hz demand

It can be observed from the figure 4.6 and figure 4.7 that the true displacement profile following the demand.

The trend of developing error with increasing the demand velocity, and the error is more than 20 percent. It is clear that the real time setup is not capable of tracking that much fast velocity with good accuracy.

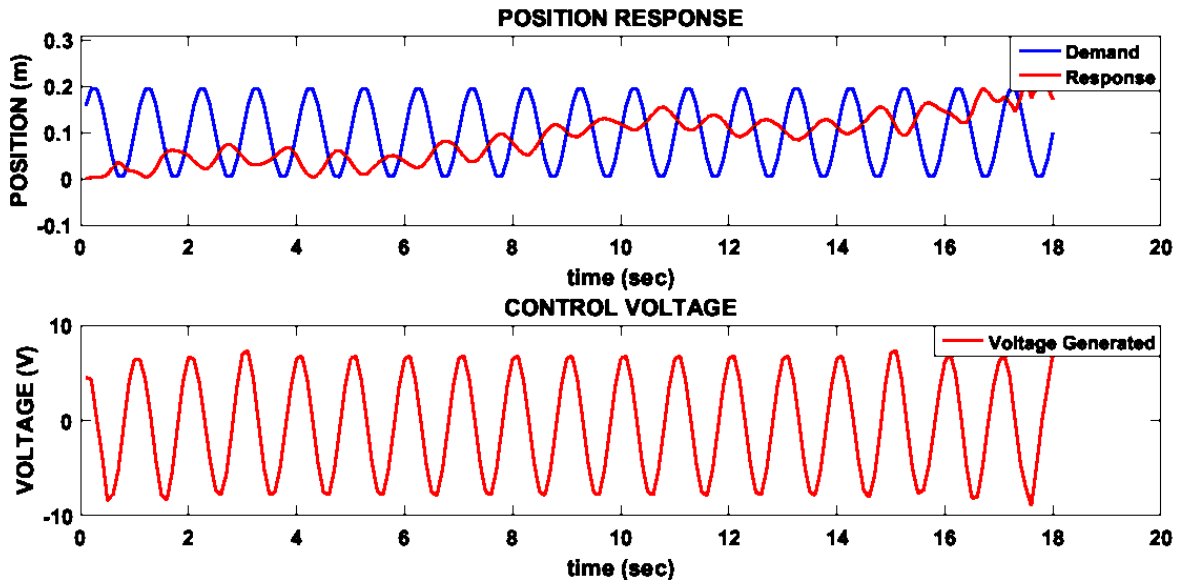


Figure 4.8 Plot of System Response for Open Loop Controller of 1 Hz demand

From figure 4.8 it is clear that the setup starts following a different trend and even it cannot trace the full stroke demand because while executing one stroke by the actuator another signal for reversing the stroke approaches towards the actuator from the controller model.

After implementing a **feed-back loop (PI) with the feed-forward controller** the response shows a better result. The results from feedforward-feedback controller at 0.1 Hz, 0.15 Hz, 0.18 Hz, 0.25 Hz, 0.3 Hz and 0.4 Hz of input frequency are shown in figure 4.9, figure 4.10, figure 4.11, figure 4.12, figure 4.13 and figure 4.14 respectively.

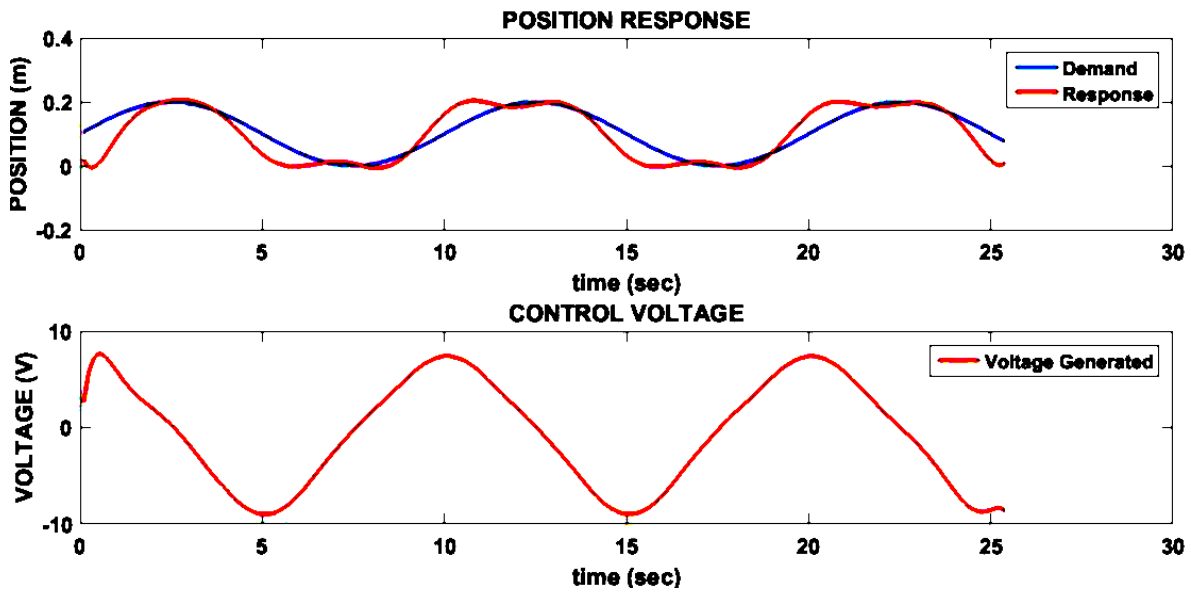


Figure 4.9 Plot of System Response for Closed Loop Controller of 0.1 Hz demand

As compare to figure 4.1, figure 4.9 shows an improvement over true response pattern while tracing the demand pattern. So it indicates that incorporation of PI feedback controller along with feedforward model gives a better response at 0.1 Hz.

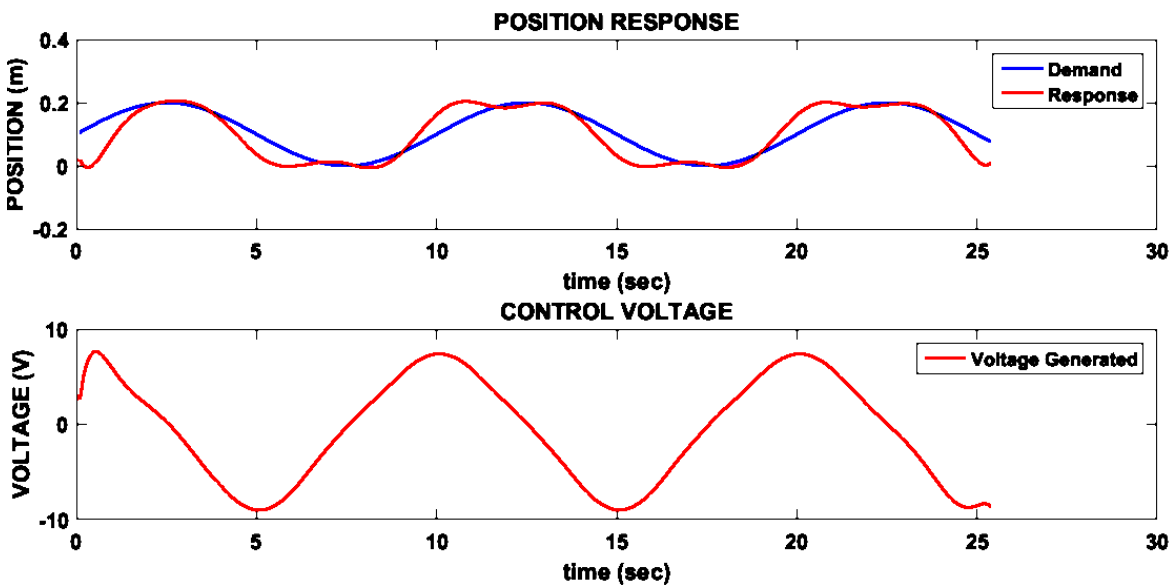


Figure 4.10 Plot of System Response for Closed Loop Controller of 0.15 Hz demand

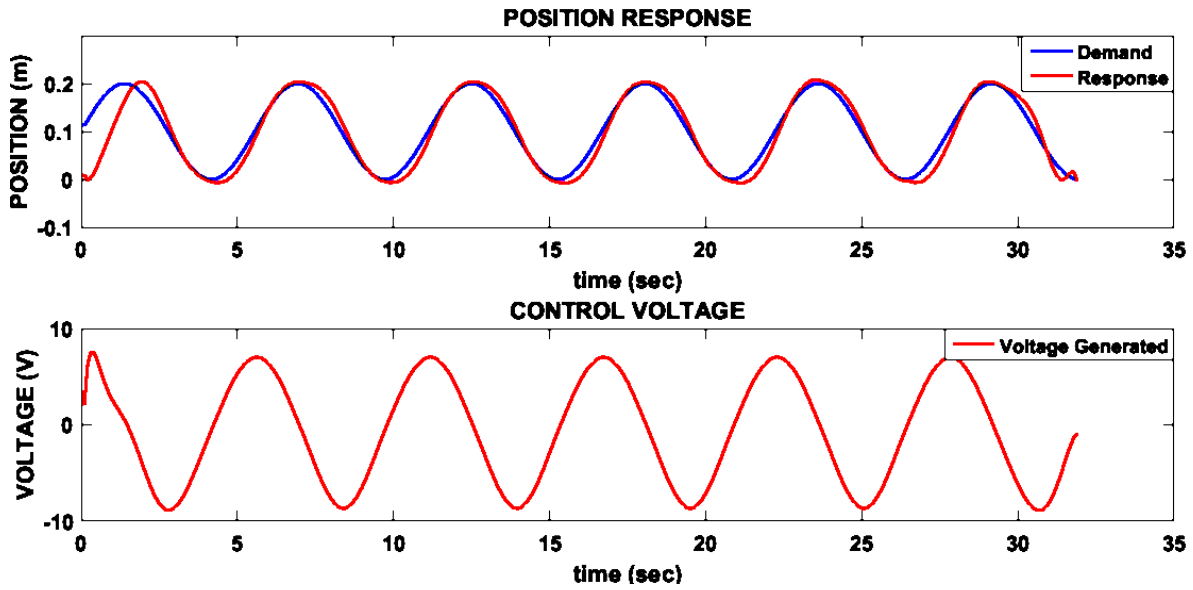


Figure 4.11 Plot of System Response for Closed Loop Controller of 0.18 Hz demand

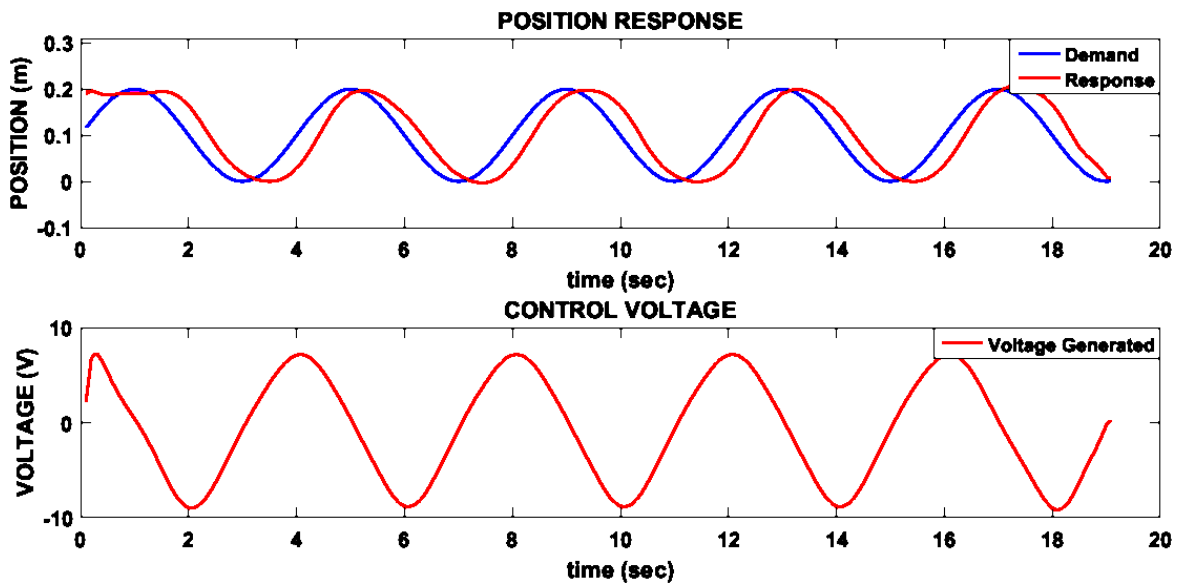


Figure 4.12 Plot of System Response for Closed Loop Controller of 0.25 Hz demand

From figure 4.11 and figure 4.12 it is observed that PI incorporation was so successful that at 0.18 Hz actual response from the real time system exactly matching with the demanded one, also it improves the response time.

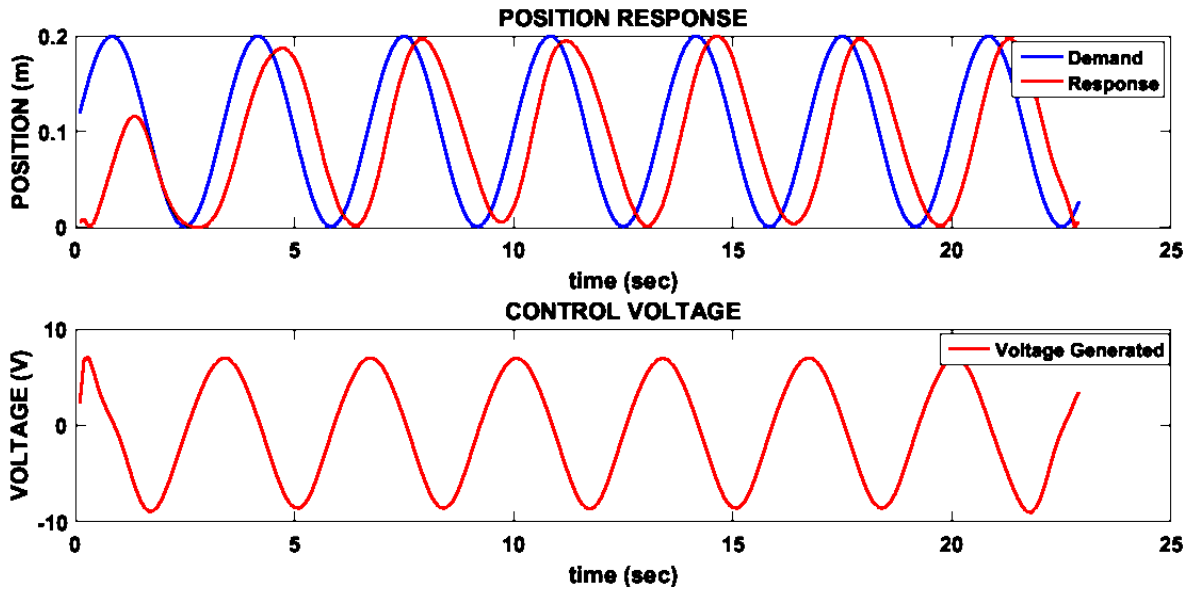


Figure 4.13 Plot of System Response for Closed Loop Controller of 0.3 Hz demand

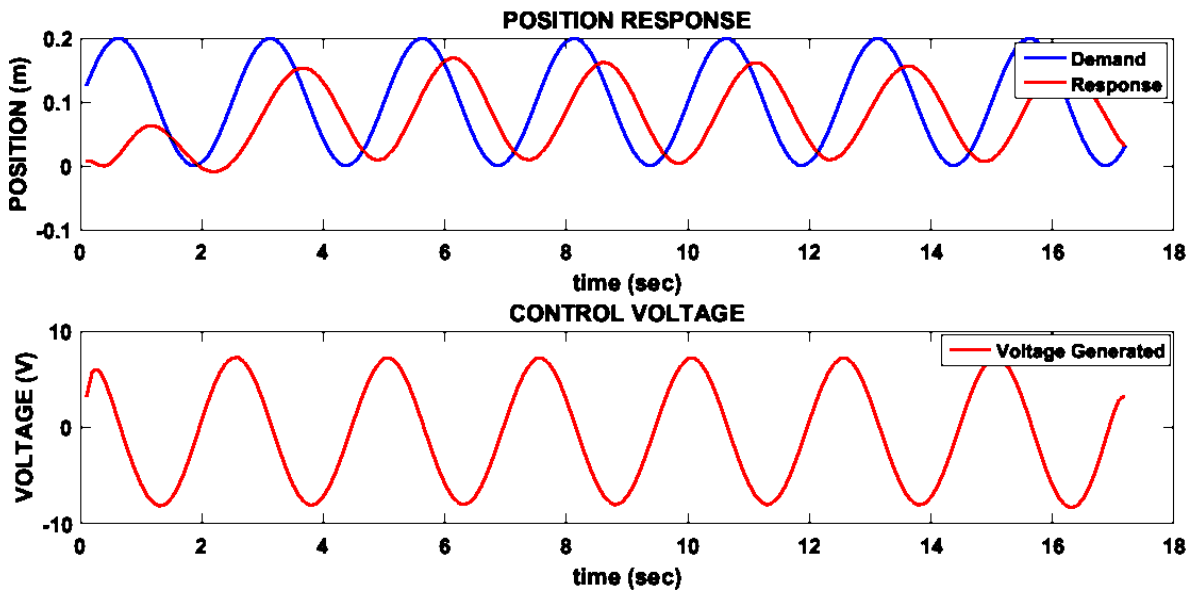


Figure 4.14 Plot of System Response for Closed Loop Controller of 0.4 Hz demand

It is clear from the above results that addition of closed loop controller improves the output response in a certain extent and it cannot trace the demanded response exactly. As compare to figure 4.5 and figure 4.6, figure 4.13 and figure 4.14 not only showing a better results in terms of error reduction but also the end retardation reduces significantly.

Some observations are made based on the above results these are as follows. This set-up gives good results at 0.15 Hz to 0.18 Hz demand frequency. At low frequency it cannot trace the demanded position properly, also at high frequency it shows a deviation from demand pattern. This deviation is quite visible at 0.25 Hz and it's huge at 0.4 Hz, and at frequency above 0.6 Hz it cannot move to its full stroke length, a middle stroke of 100 mm stroke length is the result. For very high frequency like 1 Hz or more than that, it shows completely irregular displacement pattern. Better results can be obtain by adding a PI Controller along with the feed-forward controller and the response time becomes shorter.

Chapter 5

Conclusion

And

*Future Scope of the
Work*

4.1. Conclusion

An experimental analysis has been done on EHAS which is used for providing necessary reciprocating motion to the heated MS plate in a laboratory scale ROT. Before doing the experiment, a Feed-Forward model was done in MATLAB SIMULINK to analyse compatibility of the mathematical model with the set-up. Then the model was framed in LabVIEW to carry out the experiment. The EHAS has a full functional electrohydraulic power pack. At first some analysis has been done on the EHAS by the Feed-Forward modelling only. Then a PI controller also used along with the Feed-Forward modelling, and it has been observed that this closed loop controller generates better results. The set-up gives good results in the frequency range 0.15 Hz to 0.18 Hz.

4.2. Future scope of the work

The future scope of the work could be:

- 1) In the mathematical model the values of some unknown parameters like valve coefficients, damping factor, stiffness etc. were taken from the previous experiments done on the set-up. So, if it possible to incorporate a genetic algorithm which will provide the optimised values of this unknown parameters, could be a good work.
- 2) At high frequency this set-up gives irregular outputs. So high speed cooling is a big challenge for this set-up. Making the system compatible with high speed cooling could be a good work.
- 3) Running the system with Fuzzy logic or Neural Network could be a good future work.

REFERENCES

1. Yuan G., Yu M., Wang G.D. and Liu X.H.. Heat transfer of hot strip during ultrafast cooling, *Journal of North-eastern University*, 27(4), 406-409, 2006.
2. Wang H.M., Cai Q.W., Yu W. and Su L. Effect of water flow rate on the heat transfer coefficient of a hot steel plate during laminar flow cooling, *Journal of University of Science and Technology Beijing*, 34(12) 1421-1425, 2012.
3. A.T. Hauksson. Experimental study of boiling heat transfer during sub cooled water jet impingement on flat steel surface, *Iron making & steelmaking* 31(1) 51-56, 2004.
4. Stewart I., Massingham J.D. and Hagers J.J. Heat Transfer Coefficient Effects on Spray Cooling, Presented at the 1995 AISE Annual Convention and Iron & Steel Exposition, Pittsburgh, Pennsylvania, 27th September, 1995.
5. Xu, Fuchang, and Mohamed S. Gadala. Heat transfer behaviour in the impingement zone under circular water jet, *International Journal of heat and mass transfer*, 49(21) 3785-3799, 2006.
6. Gradeck, Michel. Heat transfer from a hot moving cylinder impinged by a planar sub cooled water jet, *International Journal of Heat and Mass Transfer*, 54(25) 5527-5539, 2011.
7. Hosain M.L., Fdhila R.B. and Daneryd A. Multi-jet impingement cooling of a hot flat steel plate, *Energy Procedia*, 61, 1835-1839, 2014.
8. Hatta, Natsuo, and Hiroyuki Osakabe. Numerical modelling for cooling process of a moving hot plate by a laminar water curtain, *ISIJ International* 29(11) 919-925, 1989.
9. Samanta S., Mukherjee S., Dhar M., Barman S., Barman N., Mukhopadhyay A. and Sen S. Heat line based thermal behaviour during cooling of a hot moving steel plate using single jet, *Applied Mechanics and Materials*, 592-594, 1622-1626, 2014.
10. Wang, Bingxing. Heat transfer characteristic research during jet impinging on top/bottom hot steel plate, *International Journal of Heat and Mass Transfer* 101 844-851, 2016.
11. Wang H, Yu W, and Qingwu C. Experimental study of heat transfer coefficient on hot steel plate during water jet impingement cooling, *Journal of Materials Processing Technology*, 212(9) 1825-1831, 2012.

12. Mitra S. Study on boiling heat transfer of water–TiO₂ and water–MWCNT Nano fluids based laminar jet impingement on heated steel surface, *Applied Thermal Engineering* 37 353-359, 2012.
13. Z.D. Liu, D. Fraser, and I. V. Samarasekera. Experimental study and calculation of boiling heat transfer on steel plates during runout table operation, *Canadian metallurgical quarterly*, 41(1) 63-74, 2002.
14. Nobari, Amir Hossein, Vladan Prodanovic, and Matthias Militzer. Heat transfer of a stationary steel plate during water jet impingement cooling, *International Journal of Heat and Mass Transfer* 101 1138-1150, 2016.
15. Jizu L V. Experimental investigation of free single jet impingement using SiO₂-water Nano fluid, *Experimental Thermal and Fluid Science*, (84): 39-46, 2017.
16. Barman S, Barman N, Mukhopadhyay A and Sen S. Thermal Behaviour of a Hot Moving Steel Strip Under Multi-Cooling Jets, *Heat Transfer Engineering*, 35(14-15) 1363-1369, 2014.
17. Lyons, Oisin F P. Water mist/air jet cooling of a heated plate with variable droplet size, *Thermal Issues in Emerging Technologies, ThETA'08. Second International Conference on*. IEEE, 2008.
18. Kuraan, Abdullah M., Stefan I. Moldovan, and Kyosung Choo. Heat transfer and hydrodynamics of free water jet impingement at low nozzle-to-plate spacing's. *International Journal of Heat and Mass Transfer* 108 2211-2216, 2017.
19. Mandal P., Sarkar B K, Saha R, Chatterjee A, Mookherjee S, and Sanyal D. Real-time fuzzy-feedforward controller design by bacterial foraging optimization for an electrohydraulic system, *Engineering Applications of Artificial Intelligence*, 45, 168–179, 2015.
20. Tafazoli, Shahram, Clarence W. de Silva, and Lawrence P D. Tracking control of an electrohydraulic manipulator in the presence of friction, *IEEE Transactions on Control Systems Technology* 6(3) 401- 411, 1998.
21. Habibi R S, and Singh G. Derivation of design requirements for optimization of a high performance hydrostatic actuation system. *International Journal of Fluid Power* 1(2)11-27, 2000.

22. Sarkar B. K., Mandal P, Saha R, Mookherjee S, and Sanyal D, GA-Optimized feedforward-PID tracking control for a rugged electrohydraulic system design, *ISA Trans.* 52 853–861, 2013.
23. Guo K. Position tracking control of electro-hydraulic single-rod actuator based on an extended disturbance observer. *Mechatronics* 27 47-56, 2015.
24. Qiu H, Zhang Q, and Reid J F. Fuzzy control of electrohydraulic steering systems for agricultural vehicles, *Trans. Amer. Soc. Of Agricultural and Biol. Eng.* 44 1397– 1402, 2001.
25. Kim H M, Park S H, Song J H, Kim J S. Robust position control of electro-hydraulic actuator systems using the adaptive back-stepping control scheme *Proceedings of the Institution of Mechanical Engineers Part I- Journal of Systems and Control Engineering*, 224, 737–46, 2010.
26. Ho T and Ahn K K. Design and control of a closed-loop hydraulic energy-regenerative system, *Autom. Construction*, 22, 444–458, 2012.
27. Alleyne A and Rui Liu. A simplified approach to force control for electro-hydraulic systems, *Control Engineering Practice* 8.12, 1347-1356, 2000.
28. Qiu H and Zhang Q. Feedforward-plus-proportional–integral–derivative controller for an off-road vehicle electrohydraulic steering system, *Proc. Inst. Mech. Eng. J. Automobile Eng.*, vol. 217, 375-382, 2003.
29. Watton J and Barton R C. Further Contributions to the Response and Stability of Electrohydraulic Servo Actuators with Unequal Areas, Part 1: System Modelling. *Dynamic Systems: Modelling and Control*, ASME, NY, 155-160, 1985.
30. Chinniah Y, Burton R, Habibi S. Failure monitoring in a high performance hydrostatic actuation system using the extended kalman filter, *Int. J. Mechatronics*, 16(10), 643–53, 2006.
31. Watton J and Barton R C. Further Contributions to the Response and Stability of Electrohydraulic Servo Actuators with Unequal Areas, Part 2: Open Loop Response and Closed loop Stability, *Dynamic Systems: Modelling and Control*, ASME, NY, 161-166, 1985.
32. Wang S, Habibi S and Burton R. Sliding mode control for an electrohydraulic actuator system with discontinuous non-linear friction, *Proceedings of The Institution of*

Mechanical Engineers Part I-journal of Systems and Control Engineering, vol. 222, 799-815, 2008.

33. Kaddissi C, Kenne J P, Saad M. Indirect adaptive control of an electro-hydraulic servo system based on nonlinear back stepping, *IEEE International Symposium on Industrial electronics*, Montreal, Quebec, Canada, pp. 3147–3153, 2006.
34. Taylor C J and Robertson D. State-dependent control of a hydraulically actuated nuclear decommissioning robot, *Control Engineering Practice* 21.12 1716-1725, 2013.
35. Jun L, Yongling F, Guiying Z, Bo G, Jiming M. Research on fast response and high accuracy control of an airborne brushless DC motor, *Proceedings of 2004 IEEE International Conference on Robotics and biomimetic*, Shenyang, China, 807–810, 2004.
36. Mandal P, Sarkar B K, Saha R, Mookherjee S, Acharyya S K and Sanyal D. GA-Optimized fuzzy-feedforward-Bias control of Motion by a rugged electrohydraulic system, *IEEE/ASME Trans. Mechatronics*, vol. 20, no. 4, 1734–1742, Aug. 2015.